

MOL 25213

**CAPACITATIVE AND OAG-ACTIVATED Ca<sup>2+</sup> ENTRY DISTINGUISHED USING  
ADENYLYL CYCLASE TYPE 8**

Agnes C. L. Martin and Dermot M. F. Cooper

From the Department of Pharmacology, University of Cambridge, Tennis Court Road,  
Cambridge, CB2 1PD, United Kingdom

MOL 25213

**Running Title:** Capacitative and OAG-activated Ca<sup>2+</sup> entry pathways

**Corresponding author:** Dermot M. F. Cooper, Department of Pharmacology, University of Cambridge, Tennis Court Road, Cambridge, CB2 1PD, United Kingdom, Tel. +44 1223 334063; Fax. +44 1223 334040; E-Mail: dmfc2@cam.ac.uk

**Number of text pages:** 31

**Number of tables:** 0

**Number of figures:** 7

**Number of references:** 31

**Number of words in the Abstract:** 248 (250)

**Number of words in the Introduction:** 411 (750)

**Number of words in the Discussion:** 1259 (1500)

**List of non-standard abbreviations:** AC, adenylyl cyclase; BAPTA, 1,2-bis(o-aminophenoxy)ethane-N,N,N',N'-tetraacetic acid; BIM I, bisindolylmaleimide I; [Ca<sup>2+</sup>]<sub>i</sub>, intracellular free Ca<sup>2+</sup> concentration; cAMP, 3',5'-adenosine monophosphate; CCE, capacitative Ca<sup>2+</sup> entry; DAG, diacylglycerol; EDTA, ethylene diamine tetraacetic acid; EGTA, ethylene glycol-bis(2-aminoethylether)-N,N,N',N'-tetraacetic acid; IBMX, 3-isobutyl-1-methylxanthine; IP<sub>3</sub>, inositol 1,4,5-trisphosphate; OAG, 1-oleyl-2-acetyl-*sn*-glycerol; PKC, protein kinase C; PLC, phospholipase C; PMSF, phenylmethyl sulfonyl fluoride; SSP, staurosporine; TG, thapsigargin; TRP, transient receptor potential.

MOL 25213

## ABSTRACT

Although the molecular identity of capacitative  $\text{Ca}^{2+}$  entry (CCE) channels remains elusive, TRPC channel family members 3, 6 and 7, which are activated by diacylglycerol (DAG), have been put forward as possible candidates. As HEK 293 cells endogenously express these TRP subunits, this cell line is suitable for investigating whether DAG-activated TRP subunits form part of the putative multimeric assemblies that mediate CCE. Adenylyl cyclase type 8 (AC8) is activated by CCE in non-excitabile cells, but is not responsive to other forms of  $\text{Ca}^{2+}$  entry, such as ionophore-mediated or arachidonate-activated entry through the plasma membrane (Fagan et al., 1996; Fagan et al., 1998; Shuttleworth and Thompson, 1999). In this study, we exploited this unique dependence of AC8 on CCE to ask whether the DAG analogue, 1-oleyl-2-acetyl-*sn*-glycerol (OAG), activates the same subset of  $\text{Ca}^{2+}$  channels as store depletion, which triggers CCE. In populations of HEK 293 cells, OAG evoked a faster and greater influx of  $\text{Ca}^{2+}$  than CCE. Both pathways of  $\text{Ca}^{2+}$  entry could be triggered simultaneously in the same batch of cells, with additive effects. Strikingly, OAG-mediated  $\text{Ca}^{2+}$  entry, unlike CCE, did not stimulate AC8 activity in populations of cells. In single cells, OAG evoked a highly heterogeneous response, whereas CCE occurred as a smooth and sustained rise in  $[\text{Ca}^{2+}]_i$ . Taken together, our results indicate that, in HEK 293 cells, OAG-activated  $\text{Ca}^{2+}$  entry is distinct from CCE. The inability of the OAG-activated  $\text{Ca}^{2+}$  entry pathway to regulate AC8 further reinforces the absolute dependence of this enzyme on CCE.

Capacitative  $\text{Ca}^{2+}$  entry (CCE) is a ubiquitous mode of  $\text{Ca}^{2+}$  influx in non-excitabile cells, leading to a sustained elevation in the cytoplasmic  $\text{Ca}^{2+}$  concentration ( $[\text{Ca}^{2+}]_i$ ) (Putney, 1986). This mode of  $\text{Ca}^{2+}$  influx is activated by, and occurs after, the intracellular  $\text{Ca}^{2+}$  stores have been depleted, either by phospholipase C-linked agonists or pharmacological agents such as thapsigargin (TG). The exact mechanism which couples store depletion to CCE remains elusive, but it has recently been postulated to involve the  $\text{Ca}^{2+}$  sensor STIM1 (Zhang et al., 2005). In addition, the molecular identity of the CCE channel is far from established.

The TRPC family of channels has been suggested as likely candidates for CCE channels [for review, see (Putney, 2004)]. A closely related subset of this family, TRPC3, TRPC6 and TRPC7, can be directly activated by diacylglycerol (DAG) and its synthetic analogue 1-oleyl-2-acetyl-*sn*-glycerol (OAG) (Hofmann et al., 1999). Significantly, these DAG-activated TRP subunits are present endogenously in HEK 293 cells (Garcia and Schilling, 1997; Zagranichnaya et al., 2005).

The  $\text{Ca}^{2+}$ -stimulable adenylyl cyclase type 8 (AC8) is a focal point for cross-talk between the  $\text{Ca}^{2+}$  and cAMP signalling pathways. In non-excitabile cells, AC8 is activated by CCE and is closely associated with CCE channels. For example, BAPTA, a fast chelator of  $\text{Ca}^{2+}$ , is able to prevent AC8 stimulation by CCE, whereas at equivalent concentrations, EGTA, a slower chelating agent, is ineffective (Fagan et al., 1998). Moreover, residence of AC8 in cholesterol-rich caveolae is required for its regulation by CCE (Fagan et al., 2000; Smith et al., 2002) and contributes to the apposition of the signalling molecules of the  $\text{Ca}^{2+}$  and cAMP pathways. TRPC3 localizes to caveolae and interacts directly with caveolin-1 (Lockwich et al., 2001), thereby placing it in the same microdomain as AC8, in an ideal position to mediate CCE.

MOL 25213

Due to their close proximity to CCE channels,  $\text{Ca}^{2+}$ -stimulable adenylyl cyclases, both endogenously expressed and transiently transfected, have been shown to be selective for CCE over other types of  $\text{Ca}^{2+}$  entry, such as ionophore-mediated entry (Fagan et al., 1998). This selectivity of AC8 for  $\text{Ca}^{2+}$  entry occurring via the capacitative pathway has previously been used to discriminate between the capacitative and arachidonate-activated  $\text{Ca}^{2+}$  entry pathways in HEK 293 cells (Shuttleworth and Thompson, 1999). In this study, we asked whether OAG-activated TRP subunits might form part of the CCE apparatus, using the  $\text{Ca}^{2+}$  stimulation of AC8 as a discerning measure of CCE to determine whether OAG activates the same subset of  $\text{Ca}^{2+}$  channels as store depletion.

MOL 25213

## MATERIALS AND METHODS

*Materials* – [2-<sup>3</sup>H]adenine, [2,8-<sup>3</sup>H]cAMP, and [ $\alpha$ -<sup>32</sup>P]ATP and DNase were purchased from Amersham Biosciences (Little Chalfont, UK). Fura-2/AM and Pluronic F-127 were purchased from Molecular Probes (Paisley, UK). Thapsigargin, forskolin and 1-oleyl-2-acetyl-*sn*-glycerol was purchased from Calbiochem (Nottingham, UK). All other chemicals and culture media were purchased from Sigma (Poole, UK), BDH (Poole, UK) or Fisher Scientific (Loughborough, UK).

*Cell culture and transfection of HEK 293 cells* – Human embryonic kidney (HEK) 293 cells were cultured in minimal essential medium Eagle (MEM), supplemented with 10% fetal bovine serum, 50  $\mu$ g/ml penicillin, 50  $\mu$ g/ml streptomycin, 100  $\mu$ g/ml neomycin and 2 mM L-glutamine. Cells were maintained at 37°C in a humidified atmosphere of 5% CO<sub>2</sub>, 95% air. One day prior to transient transfection, cells were plated on 100 mm diameter dishes at ~50% confluency. The Ca<sup>2+</sup> phosphate method of transfection was adopted (Chen and Okayama, 1987) using 2  $\mu$ g of AC8 cDNA, and cells were used 2 days post-transfection.

*Measurement of [Ca<sup>2+</sup>]<sub>i</sub> in cell populations* – [Ca<sup>2+</sup>]<sub>i</sub> was measured in fura-2/AM-loaded cells using a PerkinElmer Life Sciences LS50B spectrofluorimeter. Cells were detached with phosphate-buffered saline (PBS) containing EDTA (1 mM) and loaded with fura-2/AM (2  $\mu$ M) and 0.02% Pluronic F-127 in serum-free MEM containing 20 mM HEPES and 0.1% bovine serum albumin, pH 7.4, for 30 min at room temperature. Cells were washed and resuspended in

MOL 25213

MEM. Prior to experiments,  $4 \times 10^6$  cells were resuspended in 3 ml of Krebs buffer (120 mM NaCl, 4.75 mM KCl, 1.44 mM MgSO<sub>4</sub>, 11 mM D-glucose, 25 mM HEPES adjusted to pH 7.4 with 2 M Tris base), supplemented with 0.1 mM EGTA, and transferred to a stirred cuvette. After a 1 min equilibrium interval, test substances were added from 100-fold stock solutions. The maximal ratio of fluorescence  $R_{\max}$  was determined in the presence of Triton-X (0.1% final);  $R_{\min}$  was determined in the presence of EGTA (5 mM) and Tris Base (30 mM). Fluorescence emission ratios ( $F_{340}/F_{380}$ ) were converted to Ca<sup>2+</sup> concentrations by applying the Grynkiewicz equation (Grynkiewicz et al., 1985). Mn<sup>2+</sup> quench experiments were carried out in the absence of EGTA, excitation wavelengths were set to 340 nm and 360 nm, and extracellular Ca<sup>2+</sup> was substituted for Mn<sup>2+</sup> (0.5 mM). Quantitation of peak  $[Ca^{2+}]_i$  responses was performed by averaging four independent experiments, and are shown as mean  $\pm$  S.E.M. Initial rates of Ca<sup>2+</sup> entry were calculated over a 10 second period, starting 2 seconds after the addition of extracellular Ca<sup>2+</sup>; a linear regression curve was fitted to the data and the initial rate was determined from the slope of the fitted curve (n=3). For the Gd<sup>3+</sup> block experiments, MgSO<sub>4</sub> was substituted with MgCl<sub>2</sub>, EGTA was omitted and the peak  $[Ca^{2+}]_i$  response was calculated as a percentage of the control response after subtraction of background (n=3). Statistical significance was determined using Student's t-test.

*Measurement of  $[Ca^{2+}]_i$  in single cells* – Cells were plated onto 25 mm poly-L-lysine coated coverslips 24 hours prior to loading with fura-2/AM (2  $\mu$ M) and 0.02% Pluronic F-127 for 40 min at room temperature in Krebs buffer supplemented with 1 mM CaCl<sub>2</sub>. After loading, cells were washed several times and then imaged using a CoolSNAP-HQ CCD camera (Photometrics)

MOL 25213

and monochromator system (Cairn Research, Kent, UK) attached to a Nikon TMD microscope (x40 objective). Emission images (D510/80M) at 340 nm and 380 nm excitation were collected every second using MetaFluor software (Universal Imaging). Data were plotted as 340/380 nm ratio changes relative to the fluorescence ratio prior to the addition of extracellular  $\text{Ca}^{2+}$  ( $\Delta 340/380$ ).

*Preparation of HEK 293 cell membranes* – Crude membranes were prepared from HEK 293 cells, transiently transfected with AC8 cDNA, as described previously (Nakahashi et al., 1997). Briefly, cells were sheared by passage through a 22-gauge needle, 10 times, in homogenization buffer (2 mM  $\text{MgCl}_2$ , 1 mM EDTA, 1 mM 4-(2-aminoethyl)benzenesulfonyl fluoride, 1 mM benzamidine, 1  $\mu\text{g}$  DNase, 50 mM Tris pH 7.4). Membranes were collected by centrifugation (23,000 x g, 15 min, 4°C), resuspended in assay buffer (40 mM Tris-Cl, 800  $\mu\text{M}$  EGTA, 0.25% bovine serum albumin (fraction V), pH 7.4) and stored in liquid nitrogen until use.

*Determination of Free  $\text{Ca}^{2+}$  Concentrations* – Free  $\text{Ca}^{2+}$  concentrations were established using an EGTA-buffering system as described previously (Ahljjanian and Cooper, 1987). The BAD4 computer program (Brooks and Storey, 1992) was used to estimate free  $\text{Ca}^{2+}$  concentrations by solving equations, which described the complexes formed within a mixture composed of the assay buffer components (see "Measurement of Adenylyl Cyclase Activity"). Final assay mixture concentrations of free  $\text{Ca}^{2+}$  (in the presence of 200  $\mu\text{M}$  EGTA) are shown.

*Measurement of Adenylyl Cyclase Activity* – AC8 activity was measured as described previously (Boyajian et al., 1991) with some modifications. Briefly, HEK 293 membranes (see "Preparation of HEK 293 Cell Membranes") were incubated (15 min, 30°C) in the presence of 12 mM phosphocreatine, 1.4 mM  $\text{MgCl}_2$ , 40  $\mu\text{M}$  GTP, 100  $\mu\text{M}$  cAMP, 100  $\mu\text{M}$  ATP, 25 units/ml



MOL 25213

creatine kinase, 70 mM Tris-Cl, 500  $\mu$ M isobutylmethylxanthine (IBMX), 0.5  $\mu$ Ci of [ $\alpha$ - $^{32}$ P]ATP, and  $\text{Ca}^{2+}$  (see "Determination of Free  $\text{Ca}^{2+}$  Concentrations"), in the presence and absence of 30  $\mu$ M OAG. Reactions were terminated with the addition of 100  $\mu$ l stopper solution (0.5%  $^w/v$  sodium dodecyl sulfate, 22 mM ATP, 1.5 mM cAMP), and the [ $^{32}$ P]-cAMP formed was quantified using the standard Dowex/alumina methodology and using [ $^3$ H]cAMP as a recovery marker (Salomon et al., 1974).

*Measurement of cAMP Accumulation* – Cyclic AMP accumulation in intact cells was measured as described previously (Evans et al., 1984) with some modifications (Fagan et al., 1996). HEK 293 cells were transiently transfected with AC8 and grown on 24-well plates. Cells were incubated (2 hours, 37°C) with [ $^3$ H]adenine (1.5  $\mu$ Ci/well), then washed and incubated (10 min at 30°C) in nominally  $\text{Ca}^{2+}$ -free Krebs buffer (900  $\mu$ l/well) supplemented with 0.1% bovine serum albumin. Experiments were carried out at 30°C in the presence of EGTA (100  $\mu$ M) and IBMX (100  $\mu$ M), which were preincubated with the cells for 10 min prior to a 1 min assay. Cells were treated with thapsigargin (TG; 0.1  $\mu$ M) for 4 min to empty intracellular  $\text{Ca}^{2+}$  stores prior to addition of 100  $\mu$ l assay solution (Krebs, 10  $\mu$ M forskolin,  $\text{CaCl}_2$  as shown) and terminated by addition of trichloroacetic acid (5%  $^w/v$  final). Cells were incubated on ice for at least 30 min, followed by addition of unlabelled cAMP (1  $\mu$ M), unlabelled ATP (0.65  $\mu$ M) and [ $\alpha$ - $^{32}$ P]ATP (~5,000 cpm), used as a recovery marker. After pelleting (4000 x g, 6 min), the [ $^3$ H]ATP and [ $^3$ H]cAMP content of the supernatant were quantified using the standard Dowex/alumina methodology (Salomon et al., 1974). Accumulation of cAMP is expressed as the percent conversion of [ $^3$ H]ATP into [ $^3$ H]cAMP and shown as means  $\pm$  S.D. of triplicate determinations.

## RESULTS

*Characterization of OAG-activated  $Ca^{2+}$  entry* – TRPC3, TRPC6 and TRPC7 are expressed endogenously in HEK 293 cells (Garcia and Schilling, 1997; Zagranichnaya et al., 2005). These TRP subunits are activated by DAG and its membrane-permeant synthetic analogue, OAG (Hofmann et al., 1999). It was advantageous to use OAG to activate TRP subunits in our experiments, because, unlike DAG, OAG is not metabolised to arachidonate, thereby allowing the DAG-mediated pathway to be distinguished from the arachidonate-activated pathway. Cells were suspended in nominally  $Ca^{2+}$ -free Krebs solution and treated for 1 min with a range of OAG concentrations (0 to 100  $\mu$ M). When extracellular  $Ca^{2+}$  (2 mM) was restored, a sharp increase in  $[Ca^{2+}]_i$  was evoked. The amplitude of the  $Ca^{2+}$  signal was dependent on the OAG concentration (Fig. 1A). The rise in  $[Ca^{2+}]_i$  induced by OAG was not due to CCE because during the 5 min period in which the cells were in  $Ca^{2+}$ -free medium, no depletion of the stores was observed (data not shown).

The possibility exists that OAG may exert its effects by stimulating protein kinase C (PKC) (Rozenfurt et al., 1984). To address this issue, the  $Ca^{2+}$  entry experiment in response to OAG was repeated in the presence of two PKC inhibitors, staurosporine (Fig. 1B), a broad spectrum inhibitor of protein kinases (Tamaoki et al., 1986), and bisindolylmaleimide I (Fig. 1C), which shows high selectivity for PKC isoforms  $\alpha$ ,  $\beta_1$ ,  $\beta_{II}$ ,  $\gamma$ ,  $\delta$ , and  $\epsilon$  (Toullec et al., 1991). Only in the presence of staurosporine and at the lowest concentration of OAG (30  $\mu$ M) was the peak  $[Ca^{2+}]_i$  response after treatment with OAG ( $305 \pm 51$  nM; n=4) significantly different relative to the control response in the absence of PKC inhibitor ( $196 \pm 29$  nM; n=4). High OAG concentrations produced saturating responses in HEK 293 cells, therefore a concentration of OAG of 30  $\mu$ M was used in subsequent experiments.

*OAG causes Ca<sup>2+</sup> entry through the plasma membrane.* To investigate the possibility that, rather than causing Ca<sup>2+</sup> entry, OAG may be elevating [Ca<sup>2+</sup>]<sub>i</sub> by inhibiting Ca<sup>2+</sup> extrusion or causing release from intracellular stores, a Mn<sup>2+</sup> quench experiment was carried out. Addition of extracellular Mn<sup>2+</sup> caused a leak of Mn<sup>2+</sup> into the cell, quenching the fluorescence of fura-2 at both 340 nm and 360 nm. Once the fluorescence signal was stabilised, cells were treated with TG (Fig. 2A). Release of Ca<sup>2+</sup> from intracellular stores, caused by TG, evoked an increase in fluorescence at 340 nm. On the other hand, at 360 nm, the isobestic point of fura-2, Mn<sup>2+</sup> entry through the capacitative pathway caused a decrease in fluorescence. In contrast, treatment with OAG decreased the fluorescence of fura-2 at both wavelengths, indicating that OAG is only causing Mn<sup>2+</sup> entry through the plasma membrane (Fig. 2B).

*OAG-activated Ca<sup>2+</sup> entry evokes a larger and faster increase in [Ca<sup>2+</sup>]<sub>i</sub> than CCE in populations of HEK 293 cells* – To determine whether OAG activates the same subset of Ca<sup>2+</sup> channels as those mediating CCE, the profiles of the [Ca<sup>2+</sup>]<sub>i</sub> responses arising after treatment with OAG and store depletion were compared in populations of cells. Thapsigargin (TG), a sarcoplasmic-endoplasmic reticulum calcium pump inhibitor, is routinely used to empty intracellular stores independently of receptor activation, thereby avoiding the production of DAG through the phospholipase C pathway. CCE was triggered by depleting the stores with 0.1 μM TG after 1 min equilibration in Ca<sup>2+</sup>-free Krebs (Fig. 3A). Depletion of the Ca<sup>2+</sup> stores gave rise to a modest increase in [Ca<sup>2+</sup>]<sub>i</sub>, which returned to basal level within a few minutes. At 5 min, a range of Ca<sup>2+</sup> concentrations (0 to 4 mM) were added to the extracellular medium and CCE was observed as a sharp increase in [Ca<sup>2+</sup>]<sub>i</sub>, the magnitude of which was a function of the

MOL 25213

extracellular  $[Ca^{2+}]_o$ . Although a longer incubation of TG would give rise to a larger CCE response (Fagan et al., 1998), the chosen conditions enabled OAG-activated  $Ca^{2+}$  entry to be triggered at the same time point as CCE, while minimizing passive depletion of intracellular  $Ca^{2+}$  stores.

For comparative purposes, OAG-activated  $Ca^{2+}$  entry was triggered in an analogous fashion; instead of depleting stores with TG, cells were treated for 1 min with OAG (30  $\mu$ M) (Fig. 3B). At 5 min, the same range of  $Ca^{2+}$  concentrations (0 to 4 mM) was added. Entry of  $Ca^{2+}$  by the OAG-activated pathway led to a dramatic increase in  $[Ca^{2+}]_i$ . As in the case of CCE, the amplitude of the increase in  $[Ca^{2+}]_i$  was dependent on the extracellular  $[Ca^{2+}]_o$ . Under these experimental conditions, the overall amplitude, as well as the initial rate of the  $Ca^{2+}$  entry through the OAG-activated pathway was significantly greater than for CCE (Fig. 3C).

*Low concentrations of  $Gd^{3+}$  differentially inhibit CCE and OAG-activated  $Ca^{2+}$  entry* – Since  $Gd^{3+}$  has been reported to inhibit CCE relatively specifically at low concentrations (Broad et al., 1999; Luo et al., 2001a), we investigated whether the cation could distinguish between CCE and OAG-activated  $Ca^{2+}$  entry. Although  $Gd^{3+}$  blocked both CCE (Fig. 4A) and OAG-activated  $Ca^{2+}$  entry (Fig. 4B), there was a difference in the sensitivities of the two pathways for this inhibitor. Whereas high concentrations of  $Gd^{3+}$  (5  $\mu$ M and 10 $\mu$ M) failed to discriminate between the two types of  $Ca^{2+}$  entry, at 1  $\mu$ M,  $Gd^{3+}$  was more effective against CCE than OAG-activated  $Ca^{2+}$  entry (Fig 4C). Thus,  $Gd^{3+}$  reveals subtle distinctions between the two pathways.

*OAG-activated  $Ca^{2+}$  entry has no significant effect on AC8 activity* – Using the selective activation of AC8 by CCE in non-excitable cells as a sensor for CCE, we sought to determine

MOL 25213

whether CCE and OAG-activated  $\text{Ca}^{2+}$  entry are mediated by the same channels or two distinct sets of channels. When transiently transfected in HEK 293 cells, AC8 retains its selective activation by CCE (Fagan et al., 1996) and does not affect the profiles of  $\text{Ca}^{2+}$  entry in response to TG and OAG observed in the wild type cells (data not shown). The two pathways of  $\text{Ca}^{2+}$  entry were triggered using a protocol analogous to that described for the  $[\text{Ca}^{2+}]_i$  measurement experiments. cAMP accumulation was used as a measure of AC8 activity, which was quantified during the period when  $[\text{Ca}^{2+}]_i$  increased to its maximum, in the presence of forskolin and the phosphodiesterase inhibitor, IBMX (Fig. 5A). CCE, triggered by store depletion following TG pre-treatment (0.1  $\mu\text{M}$ ), caused a robust stimulation of AC8 activity (*filled bars*, Fig. 5A). In contrast, treatment with OAG (30  $\mu\text{M}$ ) had little effect (*open bars*, Fig. 5A), even though OAG caused a greater increase in  $[\text{Ca}^{2+}]_i$  than CCE under the same conditions (see Fig. 3).

Since PKC is activated by OAG (Rozengurt et al., 1984) and inhibits another  $\text{Ca}^{2+}$ -sensitive adenylyl cyclase, AC6 (Lin et al., 2002), we sought to determine whether PKC may also inhibit AC8 and thus obscure possible stimulatory effects due to OAG-activated  $\text{Ca}^{2+}$  entry. Thus we measured cAMP accumulation, after treatment with OAG (30  $\mu\text{M}$ ), in the presence of the PKC inhibitors, staurosporine (SSP; 1  $\mu\text{M}$ ; *hatched bars*) or bisindolylmaleimide I (BIM I; 0.5  $\mu\text{M}$ ; *grey bars*), which were pre-incubated for 20 min and remained throughout the experiment. However, even in the presence of the PKC inhibitors, OAG-activated  $\text{Ca}^{2+}$  entry had little effect on AC8 activity in intact cells (Fig. 5A).

We also tested whether OAG might directly affect AC8 activity and obscure any effect of OAG-activated  $\text{Ca}^{2+}$  entry on AC8. Indeed, as OAG is membrane permeant, it could conceivably have a non-specific effect on AC8 activity. AC8 activity was measured *in vitro*, on crude membranes isolated from HEK 293 cells stably expressing AC8, in the presence of increasing concentrations

MOL 25213

of  $\text{Ca}^{2+}$  (0 to 4.5  $\mu\text{M}$ ), and in the absence and presence of OAG (30  $\mu\text{M}$ ) (Fig. 5B). The profiles of stimulation observed in each case were very similar. Therefore, OAG did not affect the ability of AC8 to be stimulated by  $\text{Ca}^{2+}$ , despite being present for longer than in the cAMP measurements.

Taken together, these results indicate that, while OAG gives rise to a  $\text{Ca}^{2+}$  entry which is greater than CCE, it has little effect on AC8 activity. Therefore AC8 clearly discriminates between CCE and OAG-activated  $\text{Ca}^{2+}$  entry. The differential ability of the two types of  $\text{Ca}^{2+}$  entry to activate AC8 indicates that different subsets of  $\text{Ca}^{2+}$  channels are involved.

*In single cells, OAG-activated  $\text{Ca}^{2+}$  entry occurs as a more heterogeneous  $[\text{Ca}^{2+}]_i$  response than does CCE* – The ability of AC8 to discriminate between CCE and OAG-activated  $\text{Ca}^{2+}$  entry indicates that these occur through distinct pathways, such that the  $[\text{Ca}^{2+}]_i$  profiles of the two responses could be expected to differ. The averaged response measured in cell populations may mask more profound heterogeneity in individual cells. Thus,  $\text{Ca}^{2+}$  measurements were performed in individual HEK 293 cells, using protocols of stimulation analogous to those used for cell population experiments. After store depletion by TG, CCE occurred immediately upon addition of 2 mM extracellular  $\text{Ca}^{2+}$  in all cells (Fig. 6A). Although cells varied in terms of the amplitude of the response, all responded with a smooth and sustained rise in  $[\text{Ca}^{2+}]_i$ . In contrast, after treatment with OAG, the addition of 2 mM extracellular  $\text{Ca}^{2+}$  caused a heterogeneous response (Fig. 6B). Strikingly, only a few cells responded immediately or simultaneously to OAG. The delay prior to the response ranged from 0 to over 7 min. In addition, the amplitude and duration of the responses varied greatly between cells. Therefore, in contrast to the sustained rise in

MOL 25213

$[Ca^{2+}]_i$  through CCE, the response to OAG was more oscillatory in nature, revealing profound differences between the two pathways in individual cells.

As different methodologies were used, the data obtained in single cells are not directly comparable to the data obtained from cell populations. However, in view of the delayed and complex response to OAG observed in many individual cells, we considered the possibility that these delayed transient rises in  $[Ca^{2+}]_i$  triggered by OAG were capable of activating AC8, but that the effect might not be detected in the first minute after addition of extracellular  $Ca^{2+}$ , when cAMP accumulation is routinely measured. Therefore cAMP accumulation was measured after treatment with TG or OAG as described previously, over a 5 minute period (Fig. 6C). Whereas CCE robustly activated AC8 at all concentrations tested, OAG-activated  $Ca^{2+}$  entry only caused a slight increase in AC8 activity at the highest concentration tested. Compared to CCE, OAG-activated  $Ca^{2+}$  entry was again ineffective.

*The  $[Ca^{2+}]_i$  rises resulting from OAG-activated  $Ca^{2+}$  entry and CCE are additive* – The fact that AC8 can distinguish between OAG-activated  $Ca^{2+}$  entry and CCE suggests that these two pathways are distinct. This argument would be strengthened if the rise in  $[Ca^{2+}]_i$  resulting from treating the same batch of cells with both TG (0.1  $\mu$ M, 4 min) and OAG (30  $\mu$ M, 1 min) was equivalent to the sum of the increases triggered by treating one batch of cells with TG and another, equivalent batch with OAG (Fig. 7A). To determine whether this is the case, leakage of  $Ca^{2+}$  into the cell, determined by adding 2 mM  $Ca^{2+}$  to untreated cells after 5 min incubation in  $Ca^{2+}$ -free Krebs, was subtracted from each of the traces corresponding to the conditions described above. The traces corresponding to the single pathways of  $Ca^{2+}$  entry, triggered in two separate populations of cells, were added (Fig. 7A, inset). The resulting trace superimposed

MOL 25213

closely with the trace corresponding to the double treatment with TG and OAG of one cell population. Therefore the  $[Ca^{2+}]_i$  rises resulting from OAG-activated  $Ca^{2+}$  entry and CCE are additive.

The effects of CCE and OAG-activated  $Ca^{2+}$  entry on AC8 activity were examined, separately and in combination (Fig. 7B). As observed previously (Fig. 5A), OAG-activated  $Ca^{2+}$  entry had little effect, whereas CCE caused a robust increase in AC8 activity. Treatment with both TG (0.1  $\mu$ M, 4 min) and OAG (30  $\mu$ M, 1 min), to trigger both pathways at once upon addition of extracellular  $Ca^{2+}$ , stimulated AC8 activity to the same degree as CCE alone. These data show that OAG-activated  $Ca^{2+}$  entry does not interfere with, or add to, the activation of AC8 by CCE.



## DISCUSSION

In non-excitabile cells, it is well established that AC8 is preferentially activated by CCE, and is unaffected by alternative forms of increase in  $[Ca^{2+}]_i$ , such as release from intracellular stores or ionophore-mediated  $Ca^{2+}$  influx (Fagan et al., 1996; Fagan et al., 1998). This property of AC8 has been successfully used to discriminate between capacitative and arachidonate-activated  $Ca^{2+}$  entry pathways (Shuttleworth and Thompson, 1999). Although the molecular identity of CCE channels remains unknown, likely candidates include the TRPC family of TRP channels, a subset of which can be activated by OAG. In this study, we explored the possibility that these OAG-activated TRP subunits may form part of the CCE apparatus by using AC8 as a sensor of CCE to determine whether OAG activates the same subset of  $Ca^{2+}$  channels as store depletion.

OAG promotes the influx of  $Ca^{2+}$  across the plasma membrane (Fig. 2), which is consistent with the presence of endogenous TRPC3, TRPC6 (Garcia and Schilling, 1997) and TRPC7 (Zagranichnaya et al., 2005) in HEK 293 cells. Furthermore, suppression of these TRPs by small interfering RNA reduces OAG-activated  $Ca^{2+}$  entry (Zagranichnaya et al., 2005). Thus it is likely that these OAG-activated TRP subunits are responsible for mediating the observed OAG-activated  $Ca^{2+}$  response. This conclusion is reinforced by the fact that OAG-activated  $Ca^{2+}$  entry is enhanced when PKC is inhibited by staurosporine (Fig. 1), which is consistent with the reported role of PKC in inhibiting TRPC3 activity in HEK 293 cells (Venkatachalam et al., 2003). Therefore PKC is not responsible for mediating the response, and on the contrary, has an inhibitory effect, such that the activation of  $Ca^{2+}$  entry in HEK 293 cells by OAG is likely to result from the direct activation of TRP subunits by OAG (Hofmann et al., 1999).

Under the chosen experimental conditions, not only was the overall magnitude of OAG-activated  $\text{Ca}^{2+}$  entry greater than that of CCE, but the rate of  $\text{Ca}^{2+}$  entry *via* the OAG-activated pathway was faster than *via* the capacitative pathway (Fig. 3). The two pathways showed different sensitivities to low concentrations of  $\text{Gd}^{3+}$ , which inhibited CCE more potently than OAG-activated  $\text{Ca}^{2+}$  entry (Fig. 4). In other cell lines, such as T-lymphocytes (Gamberucci et al., 2002) and salivary gland HSY cells (Liu et al., 2005),  $\text{Gd}^{3+}$  did not discriminate between the two pathways. Conceivably, the relative magnitude of the two pathways may impact on the potency of  $\text{Gd}^{3+}$ .

The preferential activation of AC8 by CCE was used to determine whether OAG activates the same subset of  $\text{Ca}^{2+}$  channels as store depletion. CCE robustly activated AC8, whereas OAG-activated  $\text{Ca}^{2+}$  entry had no statistically significant effect (Fig. 3). We excluded the possibility that (i) OAG-mediated activation of PKC might inhibit AC8 and mask a possible activation of the enzyme by OAG-activated  $\text{Ca}^{2+}$  entry (Fig. 3A) and that (ii) OAG, which is membrane permeant, might directly disrupt AC8 activity (Fig. 3B). Thus AC8 can discriminate between CCE and OAG-activated  $\text{Ca}^{2+}$  entry, which indicates that the two types of  $\text{Ca}^{2+}$  entry are mediated by distinct  $\text{Ca}^{2+}$  channels.

The contrasting effects of CCE and OAG-activated  $\text{Ca}^{2+}$  entry on AC8 activity led us to explore the profiles of the two pathways in single HEK 293 cells. Whereas CCE caused a sustained rise in  $[\text{Ca}^{2+}]_i$ , which occurred immediately in all cells, OAG caused a more heterogeneous response, in terms of delay, amplitude and duration. This profile is consistent with that reported in single astrocyte cells, in which OAG evoked low-frequency, high-amplitude  $[\text{Ca}^{2+}]_i$  oscillations after a brief delay (Grimaldi et al., 2003). In the individual cells, the large increases in  $[\text{Ca}^{2+}]_i$  evoked by OAG may conceivably transiently activate AC8. This may be

MOL 25213

significant in a single cell, but not in a population of cells over the short duration of the experiment. However, even extended periods after pre-treatment with OAG failed to reveal similar effects of the two modes of  $\text{Ca}^{2+}$  entry.

The selective activation of AC8 by CCE is postulated to arise from a very close apposition of the enzyme and the CCE channel (Fagan et al., 1996; Fagan et al., 1998). In addition, the localization of AC8 in cholesterol-rich caveolae is necessary for CCE regulation of AC8 (Fagan et al., 2000; Smith et al., 2002). It is possible that the channels mediating OAG-activated  $\text{Ca}^{2+}$  entry may reside in different compartments, such that the increase in  $[\text{Ca}^{2+}]_i$  caused by OAG does not occur in the vicinity of AC8. Even though both AC8 and TRPC3 have been reported to reside in lipid rafts (Fagan et al., 2000; Lockwich et al., 2001), these proteins may well segregate to separate rafts.

In HEK 293 cells, a study using small interfering RNA techniques showed that the same endogenously expressed OAG-activated TRP subunits assemble with different partners to form the complexes mediating OAG-activated  $\text{Ca}^{2+}$  entry and CCE. Thus, while TRPC1, TRPC3 and TRPC7 were found to co-assemble to mediate CCE, a complex including TRPC3, TRPC4, TRPC6 and TRPC7 was responsible for the response to OAG (Zagranichnaya et al., 2005). As our results indicate that the complexes mediating CCE and OAG-activated  $\text{Ca}^{2+}$  entry are distinct, it suggests that the TRP subunits, when part of the complex mediating CCE, are not responsive to OAG. Hence the subunits *per se* are not activated by OAG, however, in combination with specific partners, they assemble into an OAG-activated channel. If TRP subunits are recruited, by a factor such as STIM1 (Zhang et al., 2005), upon store-depletion to form CCE channels, this may account for the smooth, homogeneous response observed in all cells. In contrast, if OAG does not cause channel recruitment, this may account for the dramatic

MOL 25213

cell-to-cell variation. Moreover, the preferential activation of AC8 by CCE could be explained if the combination of subunits which assembles to form the CCE apparatus, but not the one which mediates OAG-activated  $\text{Ca}^{2+}$  entry, includes AC8 as an integral part of the complex.

The pathways mediating CCE and OAG-activated  $\text{Ca}^{2+}$  entry function independently of one another, as they can be triggered simultaneously in the same population of cells to give rise to an influx of  $\text{Ca}^{2+}$ , which is equivalent to the sum of the influxes generated through each individual pathway (Fig. 7). In this respect the OAG-activated pathway differs from the arachidonic activated pathway, which was found to potently inhibit CCE in HEK 293 cells, and *vice versa* (Luo et al., 2001b). This observation reinforces the fact that, although diacylglycerol can be metabolised to arachidonic acid, the pathways activated by each of these messengers are distinct. However, the relationship between the OAG-activated and CCE pathways appears to be cell-type specific. For example, the properties of these two pathways in T-lymphocytes are similar to those in HEK 293 cells; the effects of TG and OAG are additive, and TRPC6 has been implicated in mediating OAG-activated  $\text{Ca}^{2+}$  entry (Gamberucci et al., 2002). In contrast, a recent study in human parotid gland ductal (HSY) cells found that the effects of TG and OAG were non-additive (Liu et al., 2005). Moreover, antisense and co-immunoprecipitation experiments implicated TRPC1 and TRPC3 in mediating OAG-activated  $\text{Ca}^{2+}$  entry in these cells. Hence the relationship between CCE and OAG-mediated  $\text{Ca}^{2+}$  entry may well depend on the types of TRP channel expressed, which in turn dictates the possible combinations of TRP subunits.

In conclusion, our data show that OAG-activated  $\text{Ca}^{2+}$  entry is an independent pathway of  $\text{Ca}^{2+}$  entry in HEK 293 cells, which is mediated by channels which are distinct from the elusive CCE channels, even though they may share common TRP subunits. The inability of OAG-

MOL 25213

activated  $\text{Ca}^{2+}$  entry to regulate AC8 further reinforces the absolute dependence of this enzyme on CCE.

MOL 25213

## ACKNOWLEDGEMENTS

The authors are grateful to Dr. Debbie Willoughby for her contribution on the single cell  $\text{Ca}^{2+}$  measurements and to Dr. Tasmina Goraya, Dr. Debbie Willoughby, Nanako Masada and Rachel Simpson for their careful reading and suggestions on the manuscript.

## REFERENCES

- Ahlijanian MK and Cooper DMF (1987) Antagonism of calmodulin-stimulated adenylate cyclase by trifluoperazine, calmidazolium and W-7 in rat cerebellar membranes. *J Pharmacol Exp Ther* **241**:407-414.
- Boyajian CL, Garritsen A and Cooper DMF (1991) Bradykinin stimulates  $\text{Ca}^{2+}$  mobilization in NCB-20 cells leading to direct inhibition of adenylyl cyclase. A novel mechanism for inhibition of cAMP production. *J Biol Chem* **266**:4995-5003.
- Broad LM, Cannon TR and Taylor CW (1999) A non-capacitative pathway activated by arachidonic acid is the major  $\text{Ca}^{2+}$  entry mechanism in rat A7r5 smooth muscle cells stimulated with low concentrations of vasopressin. *J Physiol (Lond)* **517**:121-134.
- Brooks SP and Storey KB (1992) Bound and determined: a computer program for making buffers of defined ion concentrations. *Anal Biochem* **201**:119-126.
- Chen C and Okayama H (1987) High-efficiency transformation of mammalian cells by plasmid DNA. *Mol Cell Biol* **7**:2745-2752.
- Evans T, Smith MM, Tanner LI and Harden TK (1984) Muscarinic cholinergic receptors of two cell lines that regulate cyclic AMP metabolism by different molecular mechanisms. *Mol Pharmacol* **26**:395-404.
- Fagan KA, Mahey R and Cooper DMF (1996) Functional co-localization of transfected  $\text{Ca}^{2+}$ -stimulable adenylyl cyclases with capacitative  $\text{Ca}^{2+}$  entry sites. *J Biol Chem* **271**:12438-12444.
- Fagan KA, Mons N and Cooper DMF (1998) Dependence of the  $\text{Ca}^{2+}$ -inhibitable adenylyl cyclase of C6-2B glioma cells on capacitative  $\text{Ca}^{2+}$  entry. *J Biol Chem* **273**:9297-9305.

MOL 25213

Fagan KA, Smith KE and Cooper DMF (2000) Regulation of the Ca<sup>2+</sup>-inhibitable adenylyl cyclase type VI by capacitative Ca<sup>2+</sup> entry requires localization in cholesterol-rich domains. *J Biol Chem* **275**:26530-26537.

Gamberucci A, Giurisato E, Pizzo P, Tassi M, Giunti R, McIntosh DP and Benedetti A (2002) Diacylglycerol activates the influx of extracellular cations in T-lymphocytes independently of intracellular calcium-store depletion and possibly involving endogenous TRP6 gene products. *Biochem J* **364** :245-254.

Garcia RL and Schilling WP (1997) Differential expression of mammalian TRP homologues across tissues and cell lines. *Biochem Biophys Res Commun* **239**:279-283.

Grimaldi M, Maratos M and Verma A (2003) Transient receptor potential channel activation causes a novel form of [Ca<sup>2+</sup>]<sub>i</sub> oscillations and is not involved in capacitative Ca<sup>2+</sup> entry in glial cells. *J Neurosci* **23**:4737-4745.

Grynkiewicz G, Poenie M and Tsien RY (1985) A new generation of Ca<sup>2+</sup> indicators with greatly improved fluorescence properties. *J Biol Chem* **260**:3440-3450.

Hofmann T, Obukhov AG, Schaefer M, Harteneck C, Gudermann T and Schultz G (1999) Direct activation of human TRPC6 and TRPC3 channels by diacylglycerol. *Nature* **397**:259-263.

Lin TH, Lai HL, Kao YY, Sun CN, Hwang MJ and Chern Y (2002) Protein kinase C inhibits type VI adenylyl cyclase by phosphorylating the regulatory N domain and two catalytic C1 and C2 domains. *J Biol Chem* **277**:15721-15728.

Liu X, Bandyopadhyay BC, Singh BB, Groschner K and Ambudkar IS (2005) Molecular analysis of a store-operated and 2-Acetyl-sn-glycerol-sensitive non-selective cation channel: heteromeric assembly of TRPC1-TRPC3. *J Biol Chem* **280**:21600-21606.



MOL 25213

Lockwich T, Singh BB, Liu X and Ambudkar IS (2001) Stabilization of cortical actin induces internalization of transient receptor potential 3 (Trp3)-associated caveolar  $\text{Ca}^{2+}$  signaling complex and loss of  $\text{Ca}^{2+}$  influx without disruption of Trp3-inositol trisphosphate receptor association. *J Biol Chem* **276**:42401-42408.

Luo D, Broad LM, Bird GS and Putney JW Jr (2001a) Signaling pathways underlying muscarinic receptor-induced  $[\text{Ca}^{2+}]_i$  oscillations in HEK 293 cells. *J Biol Chem* **276**:5613-5621.

Luo D, Broad LM, Bird GS and Putney JW Jr (2001b) Mutual antagonism of calcium entry by capacitative and arachidonic acid-mediated calcium entry pathways. *J Biol Chem* **276**:20186-20189.

Nakahashi Y, Nelson E, Fagan KA, Gonzales E, Guillou JL and Cooper DMF (1997) Construction of a full-length  $\text{Ca}^{2+}$ -sensitive adenylyl cyclase/aequorin chimera. *J Biol Chem* **272**:18093-18097.

Putney JW Jr (1986) A model for receptor-regulated calcium entry. *Cell Calcium* **7**:1-12.

Putney JW Jr (2004) The enigmatic TRPCs: multifunctional cation channels. *Trends Cell Biol* **14**:282-286.

Rozengurt E, Rodriguez-Pena A, Coombs M and Sinnett-Smith J (1984) Diacylglycerol stimulates DNA synthesis and cell division in mouse 3T3 cells: role of  $\text{Ca}^{2+}$ -sensitive phospholipid-dependent protein kinase. *Proc Natl Acad Sci U S A* **81**:5748-5752.

Salomon Y, Londos C and Rodbell M (1974) A highly sensitive adenylyl cyclase assay. *Anal Biochem* **58**:541-548.

Shuttleworth TJ and Thompson JL (1999) Discriminating between capacitative and arachidonate-activated  $\text{Ca}^{2+}$  entry pathways in HEK 293 cells. *J Biol Chem* **274**:31174-31178.

MOL 25213

Smith KE, Gu C, Fagan KA, Hu B and Cooper DMF (2002) Residence of adenylyl cyclase type 8 in caveolae is necessary but not sufficient for regulation by capacitative  $\text{Ca}^{2+}$  entry. *J Biol Chem* **277**:6025-6031.

Tamaoki T, Nomoto H, Takahashi I, Kato Y, Morimoto M and Tomita F (1986) Staurosporine, a potent inhibitor of phospholipid/ $\text{Ca}^{2+}$ -dependent protein kinase. *Biochem Biophys Res Commun* **135**:397-402.

Toullec D, Pianetti P, Coste H, Bellevergue P, Grand-Perret T, Ajakane M, Baudet V, Boissin P, Boursier E, Loriolle F (1991) The bisindolylmaleimide GF 109203X is a potent and selective inhibitor of protein kinase C. *J Biol Chem* **266**:15771-15781.

Venkatachalam K, Zheng F and Gill DL (2003) Regulation of canonical transient receptor potential (TRPC) channel function by diacylglycerol and protein kinase C. *J Biol Chem* **278**:29031-29040.

Zagranichnaya TK, Wu X and Villereal ML (2005) Endogenous TRPC1, TRPC3 and TRPC7 proteins combine to form native store-operated channels in HEK 293 cells. *J Biol Chem* **280**:29559-29569.

Zhang SL, Yu Y, Roos J, Kozak JA, Deerinck TJ, Ellisman MH, Stauderman KA and Cahalan MD (2005) STIM1 is a  $\text{Ca}^{2+}$  sensor that activates CRAC channels and migrates from the  $\text{Ca}^{2+}$  store to the plasma membrane. *Nature* **437**:902-905.

MOL 25213

## FOOTNOTES

This work was funded by the National Institutes of Health (GM 32483) and the Wellcome Trust.

Dermot M. F. Cooper, Department of Pharmacology, University of Cambridge, Tennis Court Road, Cambridge, CB2 1PD, United Kingdom; E-Mail: dmfc2@cam.ac.uk

## FIGURE LEGENDS

**Figure 1. Characterization of OAG-activated  $\text{Ca}^{2+}$  entry in HEK 293 cells.** HEK 293 cell populations were loaded with fura-2/AM to measure changes in  $[\text{Ca}^{2+}]_i$  after pre-treatment with OAG (30  $\mu\text{M}$ , 1 min) and addition of 2 mM extracellular  $\text{Ca}^{2+}$ , in the absence (A) and presence of the PKC inhibitors, staurosporine (SSP, 1  $\mu\text{M}$ ) (B) or bisindolylmaleimide I (BIM I, 500 nM) (C). Inhibitors were pre-incubated for 20 min and present throughout the time-course. Data are representative of four independent experiments.

**Figure 2. OAG causes  $\text{Ca}^{2+}$  entry through the plasma membrane.** HEK 293 cell populations were loaded with fura-2/AM and changes in the fluorescence at 340 nm and 360 nm were measured in the presence of 0.5 mM  $\text{Mn}^{2+}$  after treatment with either TG (0.1  $\mu\text{M}$ , A) or OAG (30 $\mu\text{M}$ , C). Representative traces from three independent experiments are shown. The changes in the slope of the linear fits (*indicated*) before and after treatment with TG (B) and OAG (D) are quantified, showing the mean  $\pm$  S.E.M. of three independent experiments. \* $p < 0.05$  and \*\* $p < 0.01$ .

**Figure 3. OAG-activated  $\text{Ca}^{2+}$  entry evokes a larger and faster increase in  $[\text{Ca}^{2+}]_i$  than CCE.** A. After a 1-min equilibration period in nominally  $\text{Ca}^{2+}$ -free Krebs, cells were incubated with TG (0.1  $\mu\text{M}$ , 4 min) to empty their intracellular  $\text{Ca}^{2+}$  stores before triggering CCE by addition of 0.5, 1, 2 and 4 mM extracellular  $\text{Ca}^{2+}$ . B. Cells were incubated with OAG (30  $\mu\text{M}$ , 1 min) before adding 0.5, 1, 2 and 4 mM extracellular  $\text{Ca}^{2+}$ . Representative traces from three independent experiments are shown. C. The average  $[\text{Ca}^{2+}]_i$  at the peak response after treatment

MOL 25213

with TG or OAG and the initial rate of increase in  $[Ca^{2+}]_i$  in each case were calculated as described in 'Experimental Procedures'. The results show the mean  $\pm$  S.E.M. of three independent experiments.  $*p < 0.05$  and  $**p < 0.01$ .

**Figure 4. Low concentrations of  $Gd^{3+}$  block CCE more effectively than OAG-activated  $Ca^{2+}$  entry.** *A.* CCE was triggered in a population of HEK 293 cells loaded with fura-2/AM (2  $\mu$ M) by incubating with TG (0.1  $\mu$ M, 4 min) and adding 2 mM extracellular  $Ca^{2+}$  at 5 min, in the absence or presence of increasing concentrations of  $Gd^{3+}$  (0, 1, 5 and 10  $\mu$ M). *B.* OAG-activated  $Ca^{2+}$  entry was triggered by pretreating cells with OAG (30  $\mu$ M, 1 min) and adding 2 mM  $Ca^{2+}$  at 5 min, in the absence or presence of increasing concentrations of  $Gd^{3+}$  (0, 1, 5 and 10  $\mu$ M). Traces are representative of three independent experiments. *C.* The peak responses of  $Ca^{2+}$  entry in the presence of the different concentrations of  $Gd^{3+}$  were calculated as a percentage of the control response in the absence of inhibitor, for both TG- and OAG-treated cells. The mean  $\pm$  S.E.M. of three independent experiments are shown.  $*p < 0.05$ .

**Figure 5. OAG-activated  $Ca^{2+}$  entry has little effect on AC8 activity.** *A.* cAMP accumulation was measured in a population of HEK 293 cells transiently transfected with AC8. Activity was measured over a 1 min period, after triggering CCE (*filled bars*) or OAG-activated  $Ca^{2+}$  entry (*open bars*) as described in Fig. 2A and 2B, respectively. The effect of OAG-activated  $Ca^{2+}$  entry on AC8 was also examined in the presence of the PKC inhibitors, staurosporine (SSP; 1 $\mu$ M, 20 min preincubation; *hatched bars*) or bisindolylmaleimide I (BIM I; 500 nM, 20 min preincubation; *grey bars*). The experiments were conducted in the presence of 10  $\mu$ M forskolin. cAMP accumulation was normalised to the control in the presence of forskolin alone and the

MOL 25213

mean  $\pm$  S.E.M. of three independent experiments performed in triplicate are shown. \*\*\* $p < 0.001$  relative to controls in the absence of added  $\text{Ca}^{2+}$  in a one-way ANOVA followed by Newman-Keuls' post-test. *B.* Adenylyl cyclase activity was determined in membranes prepared from HEK 293 cell expressing AC8, in the absence (*filled circles*) or presence (*open circles*) of 30  $\mu\text{M}$  OAG. The experiments were conducted in the presence of 1  $\mu\text{M}$  calmodulin and the estimated concentrations of free  $\text{Ca}^{2+}$  shown. The results show the means  $\pm$  S.D. of triplicate determinations, fitted to a sigmoidal dose-response curve using GraphPad Prism (GraphPad Software, Inc.). The concentration of free  $[\text{Ca}^{2+}]_i$  causing half-maximal AC8 activity, as well as the maximal level of AC8 activity did not differ significantly between the two conditions in a Student's t-test.

**Figure 6. OAG-activated  $\text{Ca}^{2+}$  entry causes a more heterogeneous  $[\text{Ca}^{2+}]_i$  response than CCE in single cells.**  $[\text{Ca}^{2+}]_i$  was measured in single cells after addition of extracellular  $\text{Ca}^{2+}$  in response to treatment with TG (0.1  $\mu\text{M}$ , 4 min; *A*) or OAG (30  $\mu\text{M}$ , 1 min; *B*). For comparative purposes, the  $[\text{Ca}^{2+}]_i$  signal was normalised to the level prior to addition of extracellular  $\text{Ca}^{2+}$ . In view of the delayed response to OAG in many cells, cAMP accumulation was measured over a 5 min period (*C*), after triggering CCE (*filled bars*) or OAG-activated  $\text{Ca}^{2+}$  entry (*open bars*) as described in Fig. 3. Data are plotted as mean  $\pm$  S.D. of triplicate determinations. \* $p < 0.05$  and \*\*\* $p < 0.001$  relative to controls in the absence of added  $\text{Ca}^{2+}$  in a one-way ANOVA followed by Newman-Keuls' post-test.

**Figure 7. The effects of OAG-activated  $\text{Ca}^{2+}$  entry and CCE are additive.** *A.* CCE was triggered in a population of HEK 293 cells loaded with fura-2/AM (2  $\mu\text{M}$ ) by incubating with

MOL 25213

TG (0.1  $\mu\text{M}$ , 4 min) and adding 2 mM extracellular  $\text{Ca}^{2+}$  at 5 min. OAG-activated  $\text{Ca}^{2+}$  entry was triggered by pretreating cells with OAG (30  $\mu\text{M}$ , 1 min) and adding 2 mM  $\text{Ca}^{2+}$  at 5 min. Both types of  $\text{Ca}^{2+}$  entry were triggered simultaneously by treating with TG (0.1  $\mu\text{M}$ , 4 min) and OAG (30  $\mu\text{M}$ , 1 min) before adding 2 mM  $\text{Ca}^{2+}$  at 5 min. As a control, the basal leak of  $\text{Ca}^{2+}$  into untreated cells upon addition of 2mM extracellular  $\text{Ca}^{2+}$  was measured. The basal leak of  $\text{Ca}^{2+}$  into cells was subtracted from the traces corresponding to CCE, OAG-activated  $\text{Ca}^{2+}$  entry, and both types of  $\text{Ca}^{2+}$  entry combined (*inset*). Traces corresponding to CCE and OAG-activated  $\text{Ca}^{2+}$  entry were then added and compared to the trace corresponding to the simultaneous entry of  $\text{Ca}^{2+}$  through the capacitative and OAG-activated pathways. *B.* AC8 activity measurements in response to the CCE pathway alone, the OAG-activated  $\text{Ca}^{2+}$  entry alone, and the combination of both CCE and OAG-activated  $\text{Ca}^{2+}$  entry in the same sample. \*\*\* $p < 0.001$  relative to controls in the absence of added  $\text{Ca}^{2+}$  in a one-way ANOVA followed by Newman-Keuls' post-test; n.s. indicates that the stimulation of AC8 activity by treatment with both TG and OAG is not significantly different ( $p > 0.05$ ) from that resulting from CCE alone.

## FIGURES

### FIGURE 1

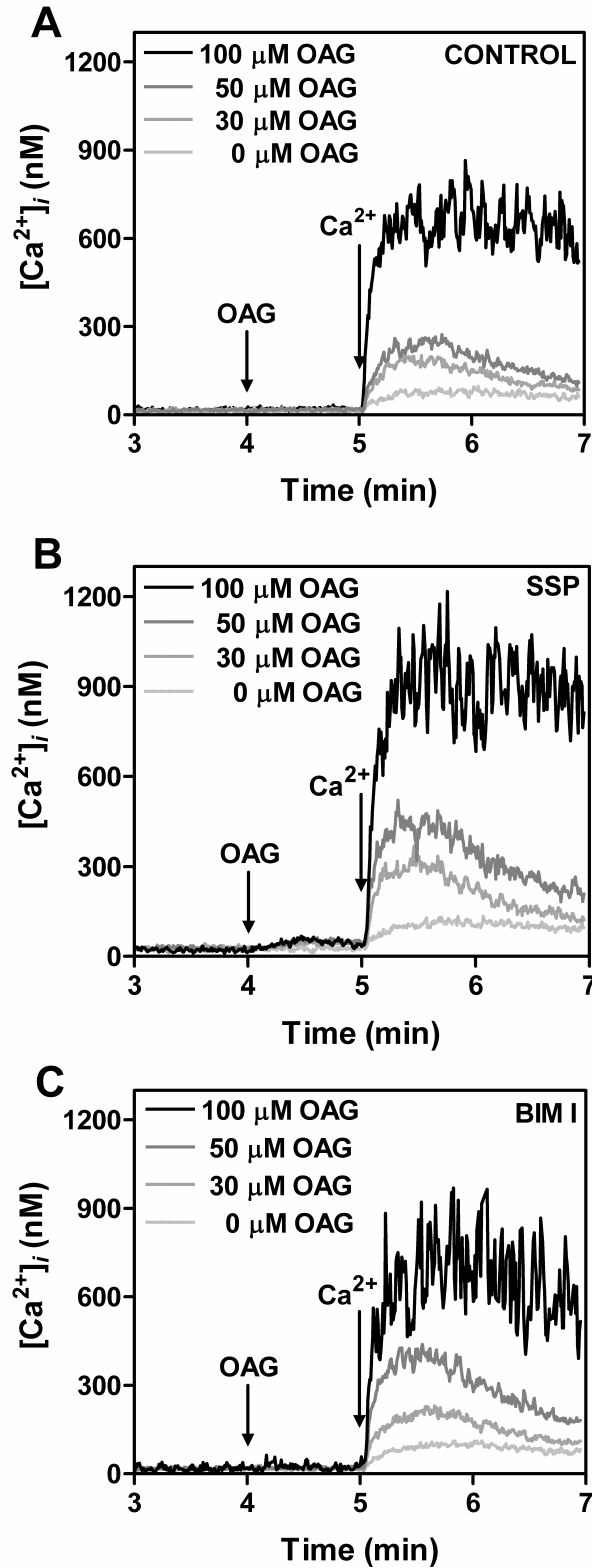




**FIGURE 2**

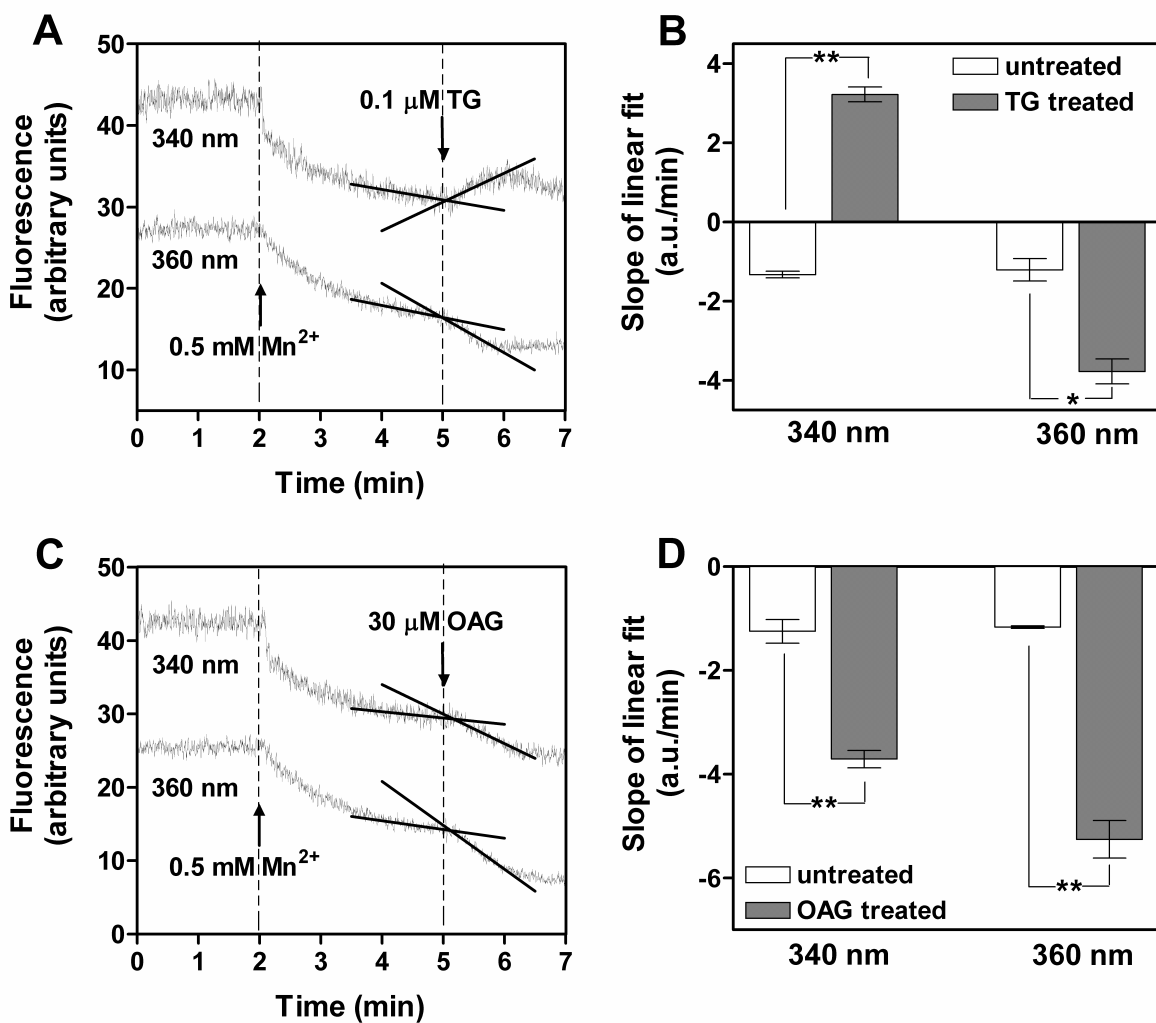


**FIGURE 3**

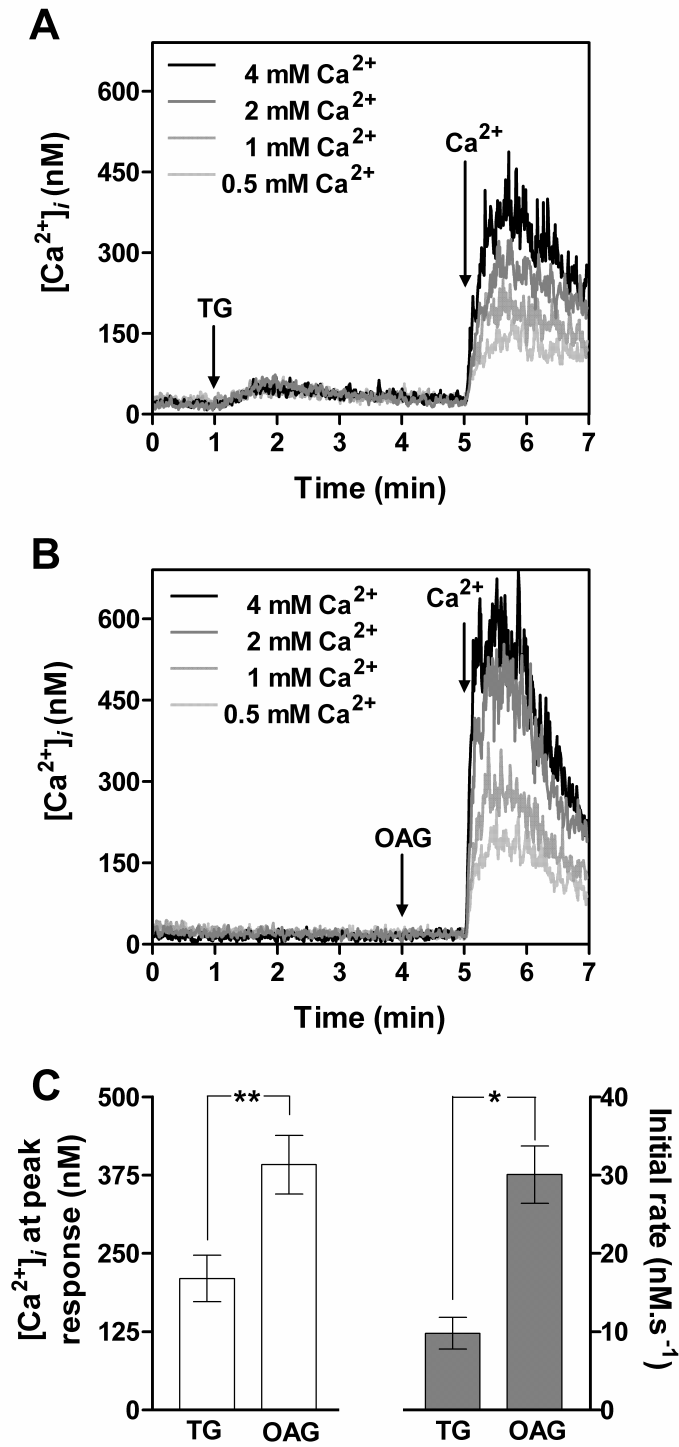


## FIGURE 4

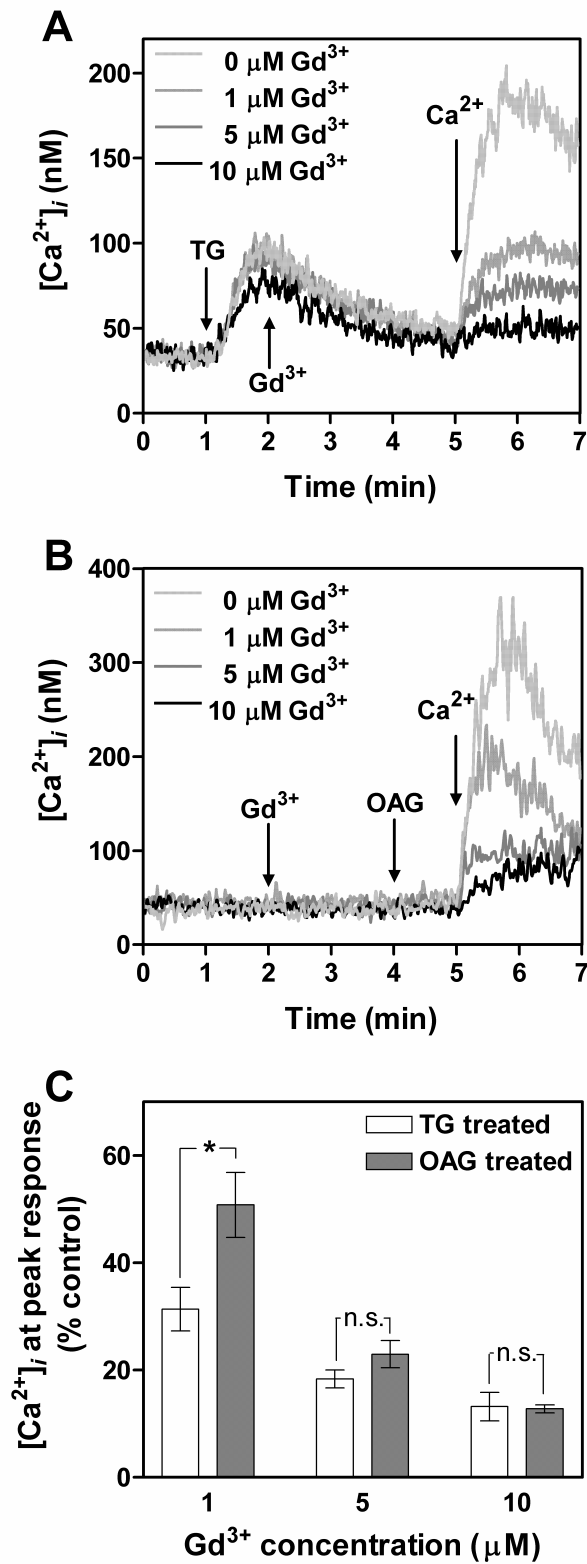
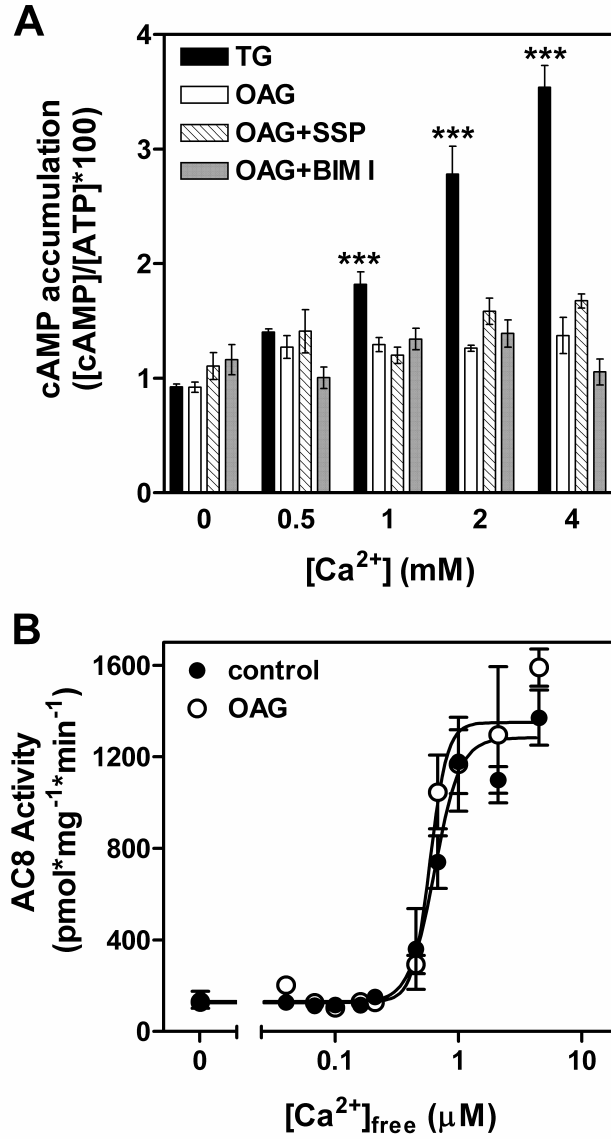


FIGURE 5



**FIGURE 6**

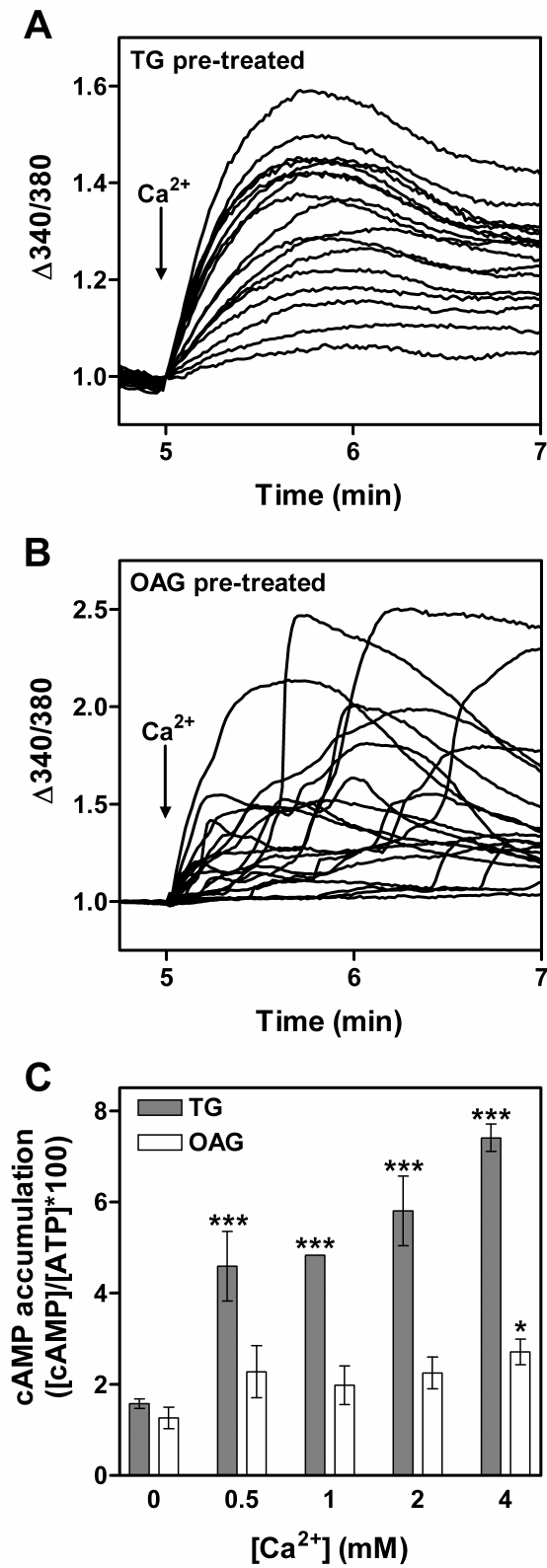


FIGURE 7

